Effects of graphene imperfections on the structure of self-assembled pentacene films



2015 J. Phys. D: Appl. Phys. 48 395304

(http://iopscience.iop.org/0022-3727/48/39/395304)

IOP Publishing Journal of Physics D: Applied Physics
J. Phys. D: Appl. Phys. **48** (2015) 395304 (7pp) doi:10.1088/0022-3727/48/39/395304

# Effects of graphene imperfections on the structure of self-assembled pentacene films

**W Jung[1], S J Ahn[1], S Y Lee[1], Y Kim[1], H-C Shin[1], Y Moon[1], S H Woo[2], C-Y Park[1] and J R Ahn[1,3]**

[1] Department of Physics, Sungkyunkwan University, Suwon 440–746, Korea
[2] College of Pharmacy, Chungnam National University, Daejeon 305–764, Korea
[3] SAINT, Sungkyunkwan University, Suwon 440–746, Korea

E-mail: cypark@skku.edu and jrahn@skku.edu

Received 1 June 2015, revised 6 August 2015
Accepted for publication 11 August 2015
Published 4 September 2015


**Abstract**

The quality of pentacene films in pentacene-based devices significantly affects their performance. In this report, the effects of various defects in graphene on a pentacene film were studied with scanning tunneling microscopy. The two most common defects found in the epitaxial graphene grown on SiC(0 0 0 1) substrates were subsurface carbon nanotube (CNT) defects and step edges. The most significant perturbation of the pentacene films was induced by step edges between single-layer and bilayer graphene domains, while the effect of step edges between single-layer domains was marginal. The subsurface CNT defects slightly distorted the structure of the single-layer pentacene, but the influence of such defects decreased as the thickness of the pentacene film increased. These results suggest that the uniformity of the graphene layer is the most important parameter in the growth of high-quality pentacene films on graphene.

Keywords: pentacene, graphene, scanning tunneling microscopy

(Some figures may appear in colour only in the online journal)

## 1. Introduction

Graphene, a one-atom-thick planar structure of $sp^2$-bonded carbon atoms, is considered an emerging material because of its outstanding mechanical and electronic properties [1–4]. In particular, its high optical transparency, high charge-carrier mobility, and low sheet resistance have led it to be considered a potential electrode material for optoelectronic devices [5], such as organic light-emitting diodes [6, 7], organic field-effect transistors [8–13], and organic photovoltaic devices [14, 15]. Of the various organic molecules available, pentacene ($C_{22}H_{14}$) is of particular interest because thin films containing pentacene have shown remarkably high charge-carrier mobilities [16, 17]. Furthermore, because of its simple structure, pentacene has become one of the most popular organic molecules for organic devices. Recent studies have demonstrated that pentacene films are compatible with graphene, and excellent performances have been achieved with graphene-based organic devices [9–13].

For efficient charge transport in organic semiconductors, charges must move from molecule to molecule without being trapped or scattered. The charge-carrier mobility is influenced by several factors, including the molecular packing and orientation [18]. The intermolecular transfer integral, a key charge transport parameter that expresses the ease with which charges are transferred between adjacent molecules, is extremely sensitive to the molecular arrangement and is based on the hopping conduction mechanism of organic semiconductors [19]. The packing of organic molecules on a substrate is determined by the relative strength of the intermolecular interactions compared to the molecule–substrate interactions [20]. The packing of organic molecules can also be affected by any imperfections in the substrate, such as defects or step edges [21, 22]. Therefore, to understand the packing of organic molecules on a substrate, it is essential to study the interactions of the organic molecules with both uniform and non-uniform substrates.

Scanning tunneling microscopy (STM) has been used to study the effects of the interactions between various organic molecules and graphene on their self-assembled molecular packing, including perylene-3,4,9,10-tetracarboxylic

 

dianhydride (PTCDA) [17–19], perylene tetracarboxylic diimide [25, 26], 7,7′,8,8′-tetracyano-p-quinodimethane [27, 28], metal phthalocyanines [29, 30], and pentacene [31]. In particular, the interfacial structure between a pentacene film and graphene has been focused on and investigated with photoemission spectroscopy [32], 2D grazing incidence diffraction, and near-edge x-ray absorption fine-structure spectroscopy [13]. However, the relationships between the non-uniformity of the graphene and self-assembly of the pentacene molecules were not clearly understood at molecular scale [33–35].

In this study, we investigated how the structure of self-assembled pentacene films on imperfect graphene substrates deviate from that on uniform graphene substrates. The self-assembled pentacene films on the defect-containing graphene substrates were imaged with STM at room temperature. The pentacene films were grown on graphene that was epitaxially grown on 6H-SiC(0 0 0 1) substrates. The epitaxial graphene contained subsurface carbon nanotube (CNT) defects, six-fold scattering-centre defects, and step edges [23, 36, 37]. The CNT defects slightly disturbed the arrangement of the flat-lying arrangement, while the continuous growth of the flat-lying arrangement was maintained. In contrast to the CNT defects, the step edges between single-layer and bilayer graphene domains significantly interrupted the continuous growth. The step edges between the different graphene layers were approximately 0.35 nm in height and limited the continuous packing of the pentacene molecules, while the step edges between the single-layer graphene domains had a height of 0.25 nm and did not disturb the formation of the pentacene films.

## 2. Experiment

The epitaxial graphene was grown on 6H-SiC(0 0 0 1) substrates in an ultra-high vacuum (UHV) chamber equipped with an STM chamber. Before growing the graphene, the SiC substrates were etched in a $H_2$ atmosphere to obtain a flat surface and then loaded into the UHV chamber. The SiC substrates were exposed to a Si flux while heated at 850 °C to produce a clean surface, which resulted in a Si-terminated $3 \times 3$ surface that was observed with low-energy electron diffraction. The Si-terminated surface was heated to high temperatures without the Si flux to grow the epitaxial graphene. Zero-layer, single-layer, and bilayer graphene were grown at temperatures of 1050 °C, 1200 °C, and 1300 °C, respectively. In this study, we used single-layer graphene without the zero-layer graphene because it has been reported that pentacene films do not form an ordered film on zero-layer graphene [31]. The single-layer graphene coexisted with the bilayer graphene, which is inevitable because of the higher Si sublimation rates at the step edges [38]. The presence of single-layer graphene was always confirmed with STM before the adsorption of the pentacene molecules was performed. The pentacene was evaporated from a resistively heated graphite crucible that was outgassed overnight in the UHV chamber. During the deposition of pentacene, the substrate was kept at RT and the pressure was maintained below $5.0 \times 10^{-10}$ Torr, with the baseline pressure $= 7.0 \times 10^{-11}$ Torr. The STM images were obtained at RT with a commercially available, variable-temperature STM (Omicron, Germany) in constant current mode, and electrochemically etched tungsten tips were used.

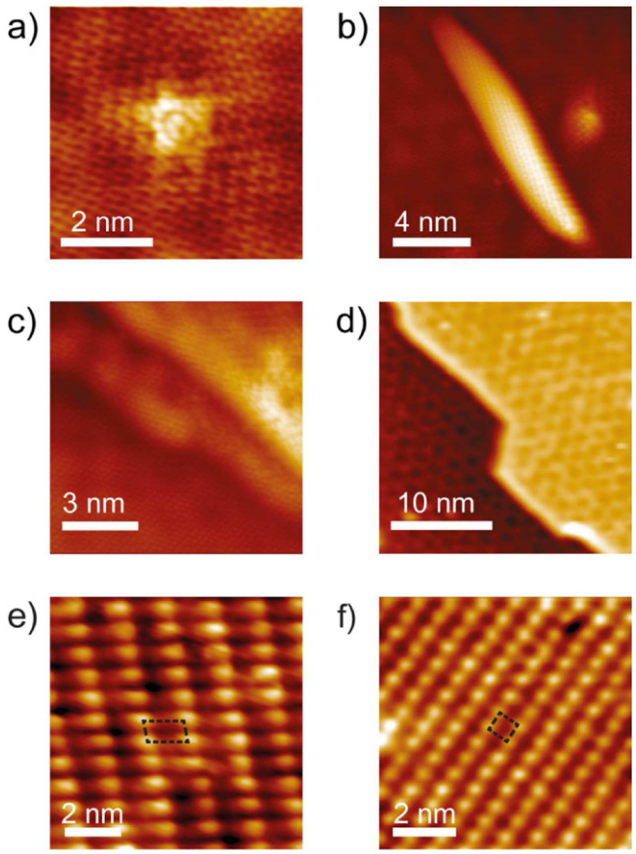


**Figure 1.** STM images of epitaxial graphene with various imperfections (a)–(d) and the self-assembled pentacene molecules (e), (f). (a) An STM image ($V_s = -0.1$ V) of a six-fold scattering-centre defect. (b) An STM image ($V_s = -0.1$ V) of a subsurface CNT defect. (d) An STM image ($V_s = -0.1$ V) of a step edge between single-layer graphene domains. (d) An STM image ($V_s = -0.1$ V) of a step edge between single-layer and bilayer graphene domains. (e) An STM image ($V_s = +1.6$ V) of the flat-lying structure of the pentacene molecules. (f) An STM image ($V_s = +2.5$ V) of the herringbone structure of the pentacene molecules.

## 3. Results and discussion

Four different types of imperfections were observed in the single-layer graphene. Figure 1(a) shows a six-fold scattering-centre defect. These defects are formed by the movement of graphene fragments, which produces five- or seven-membered rings [39]. Figure 1(b) shows a subsurface CNT defect. It has been reported that the CNT defects are formed by the folding of incomplete graphene pieces, and the formation is driven by the thermodynamics and saturation of the opposite edges that possess dangling bonds near the subsurface SiC structures during the graphitization [37, 40]. Figure 1(c) shows a step edge between single-layer graphene domains, while figure 1(d) shows step edges between single-layer and bilayer

graphene domains, as reported previously [36]. Figure 1(e) shows the flat-lying arrangement of pentacene molecules that was observed when pentacene molecules formed a single layer [31]. With a thicker pentacene layer, the pentacene molecules prefer a standing-up arrangement called a herringbone structure, as shown in figure 1(f) [31, 41, 42].

The effects of the graphene defects on the pentacene arrangement were further studied. Three representative imperfections of epitaxial graphene were considered: a subsurface CNT defect, a step edge between single-layer and bilayer graphene domains, and a step edge between single-layer graphene domains. The line profile across the six-fold scattering-centre defect, as shown in figures 2(a) and (c), indicates that its height is approximately 0.05 nm. In comparison to the six-fold scattering-centre defect, the heights of the CNT defects in the STM image are above 0.2 nm, where the dot-shaped CNT defect has a height of approximately 0.2 nm and the long CNT defect is approximately 0.5 nm in height. The line profiles suggest that the height can be used to distinguish the types of defects. The line profiles across the defects of the pentacene films show that the heights are approximately 0.2 nm, as shown in figures 2(e)–(h), which is quite consistent with the height of the dot-shaped CNT defect in figure 2(b). The line profiles suggest that the defects underlying the pentacene films can be assigned to a dot-shaped or a short CNT defect. As can be seen in figures 2(e) and (f), the subsurface CNT defects distort the flat-lying arrangement, but do not affect the herringbone structure. For PTCDA, it has been reported that the subsurface CNT defects do not disturb the self-assembled flat-lying arrangement of PTCDA molecules [23]. This difference between the pentacene and PTCDA molecules suggests that the effects of subsurface CNT defects on the self-assembled structure of organic molecules may be related to the different interactions between the organic molecules and graphene. PTCDA has more aromatic rings than pentacene, and therefore, may have stronger interactions with graphene, meaning that the PTCDA arrangement is less perturbed by the subsurface CNT defects. For the herringbone structure, it is only observed in thicker pentacene films. Hence, it is natural that the effects of the subsurface CNT defects on a pentacene film decrease as the film thickness increases.

Single-layer graphene coexists with bilayer graphene because the Si atoms at the step edges are sublimated more than those in the terraces [38]. As described above, we studied two different types of step edges: the step edge between single-layer graphene domains and the step edge between single-layer and bilayer graphene domains. Figure 3(a) shows the different structures of the pentacene film at the step edges. The flat-lying structure of the pentacene molecules has grown through the step edge denoted S1 in figures 3(a) and (b), which we will call a step-crossing arrangement hereafter. The step-crossing arrangement is consistent with previous reports of PTCDA and pentacene [23, 24, 43]. In contrast to the step-crossing arrangement, the flat-lying structure is affected by the step edge denoted S2 in figures 3(a) and (c), and the pentacene grows along the step edge, which we will call a step-following arrangement hereafter. The step-following arrangement was observed first in this study, and it has a different unit cell

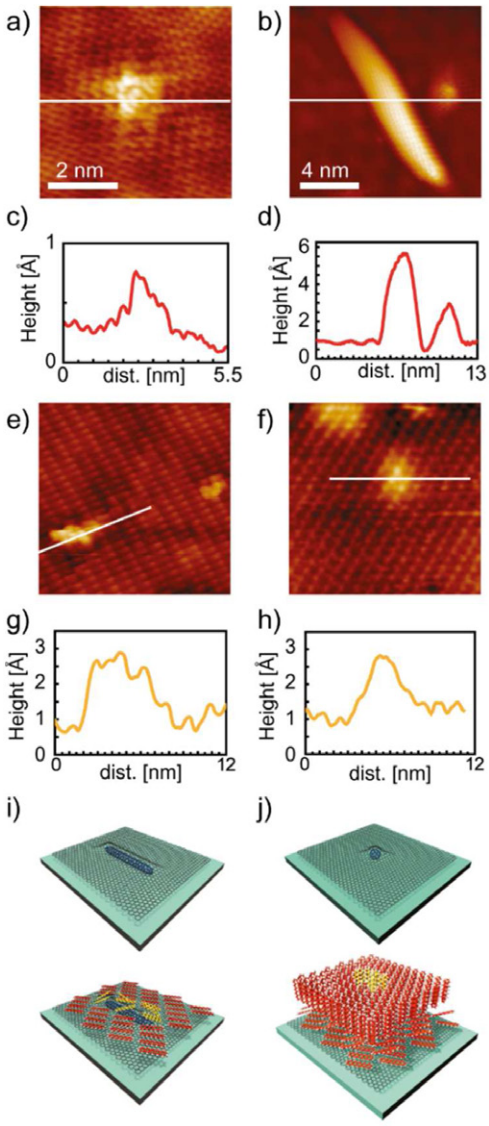


**Figure 2.** Line profiles across defects. (a), (c) Line profiles across the six-fold scattering-centre defect. (b), (d) Line profiles across the subsurface CNT defect. (e), (g) An STM image ($V_s = +1.6$ V) and its line profile of the flat-lying structure on a subsurface CNT defect. (f), (h) An STM image ($V_s = +2.5$ V) and its line profile of the herringbone structure on a subsurface CNT defect. (i), (j) Molecular structure models of the (i) flat-lying and (j) herringbone structures on the subsurface CNT defects, where the red, black, and blue structures represent the pentacene molecules, graphene, and subsurface CNT defects, respectively. The yellow structures indicate the pentacene molecules located on the subsurface CNT defects.

($\vec{a} = 1.84 \pm 0.05$ nm, $\vec{b} = 0.73 \pm 0.05$ nm, and $\gamma = 76° \pm 3°$) compared to that of the step-crossing arrangement; the $\vec{a}$ vector is longer than that of the step-crossing arrangement [31]. Furthermore, another difference is that the pentacene molecules grow along the step edge, and thus, the orientation of the pentacene molecules is not related to the orientation of the underlying graphene. This arrangement is also different from that reported for pentacene molecules grown on a vicinal Cu surface, Cu (1 1 9) [44, 45]. The pentacene molecules on a Cu (1 1 9) substrate also grow along the step edges, but their long molecular axis is parallel to the step edge. In

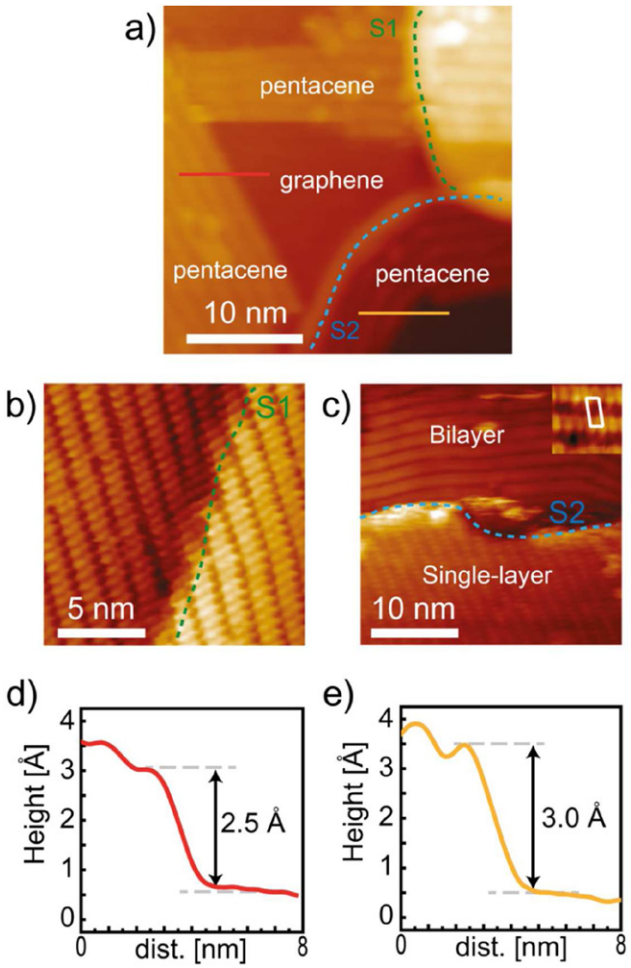


**Figure 3.** The effects of step edges on the arrangement of pentacene molecules. (a) An STM image ($V_s = +3.0$ V) of the flat-lying structure of the pentacene molecules near step edges, with the pentacene molecules and epitaxial graphene highlighted. (b) A STM image ($V_s = +1.6$ V) of the flat-lying structure, where S1 indicates a step edge between single-layer graphene domains. (c) A STM image ($V_s = +1.6$) of the flat-lying structure, where S2 indicates a step edge between single-layer and bilayer graphene domains. The inset in (c) shows an enlarged STM image of the step following arrangement and its unit cell. (d), (e) Line profiles of pentacene films in (a), where the positions of the line profiles in (a) are indicated by the same color lines. Here, we note that the STM images in (b) and (c) were obtained at different regions from the one of (a).

contrast to the vicinal Cu surface, the long molecular axis of the pentacene molecules on the epitaxial graphene (see the upper terrace and inset in figure 3(c)) is perpendicular to the step edge. To determine the number of layers of pentacene films, the line profiles across the boundaries of the pentacene films were obtained, as shown in figures 3(d) and (e), where the boundaries are indicated by the lines in figure 3(a). The line profile of the step-crossing arrangement shows that the height of the pentacene film is approximately 0.25 nm (see figure 3(d)), while the height of the pentacene film with the step-following arrangement is approximately 0.3 nm (see figure 3(e)). The height difference is only 0.05 nm, which suggests that both the pentacene films have the same number of layers. In the previous report of pentacene molecules on graphite [46], the height of a single-layer pentacene film with the flat-lying structure was 0.22 nm. Here we note that the STM images in the previous report of pentacene molecules on graphite are filled-state, while the STM images in this report are empty-state. These results suggest that both the pentacene films with the step-crossing and step-following arrangements are single-layer.

To understand the differences between the step-crossing and step-following arrangements, we measured line profiles across the step edges to determine the step heights, as shown in figure 4. Figure 4(e) shows that the step height is 0.26 nm for the step-crossing arrangement, while figure 4(f) shows that the step height is 0.34 nm for the step-following arrangement. The epitaxial single-layer graphene domains can coexist with zero-layer or bilayer graphene domains. It has been reported that pentacene molecules do not form an ordered phase on the zero-layer graphene, and thus, the formation of zero-layer graphene can be excluded [31, 34]. For this reason, there are two different types of graphene: single-layer and bilayer graphene. Under the preparation conditions used in this study, the single-layer graphene is dominant, as observed with STM. Hence, step edges can be formed between single-layer graphene domains (a single-layer step edge) or between single-layer and bilayer graphene domains (a bilayer step edge). Many groups have reported that the step height between single-layer graphene domains is 0.25 nm, while the step height between single-layer and bilayer graphene domains is 0.34 nm [36, 47–49]. Because a single graphene layer is formed by the sublimation of Si atoms from three SiC layers, the height difference between underlying SiC layers of single-layer and bilayer graphene is equivalent to the height of three SiC layers that is 0.75 nm, as indicated in figure 4(b). Furthermore, the interlayer distance between graphene layers is 0.34 nm so that the height difference between single-layer and bilayer graphene is 0.41 nm from the point of view of the atomic structure. These step heights suggest that the step-crossing and step-following arrangements occur at single-layer and bilayer step edges, respectively. These results also suggest that the long molecular axis of pentacene molecules on the bilayer graphene (see the upper terrace in figure 3(c)) is perpendicular to the step edge. In contrast to the bilayer graphene, the long molecular axis of pentacene molecules on the single-layer graphene (see the lower terrace in figure 3(c) and the upper and lower terraces in figure 3(b)) inclines to the step edge [31]. Pentacene molecules on bilayer graphene prefer the step-following arrangement so that the long molecular axis of pentacene molecules is always perpendicular to the step edge. For single-layer graphene, the long molecular axis of pentacene molecules prefers to be aligned with the zigzag edge of graphene but makes an angle of 30° with the armchair edge, as reported previously [31].

The height of the pentacene film with the step-following arrangement on bilayer graphene is higher than that of the pentacene film with the step-crossing arrangement on single-layer graphene, where both the pentacene films are single-layer. The height difference suggests that the interactions of pentacene molecules with graphene are stronger on single-layer graphene than on bilayer graphene. Furthermore, the interactions are stronger on zero-layer graphene than on

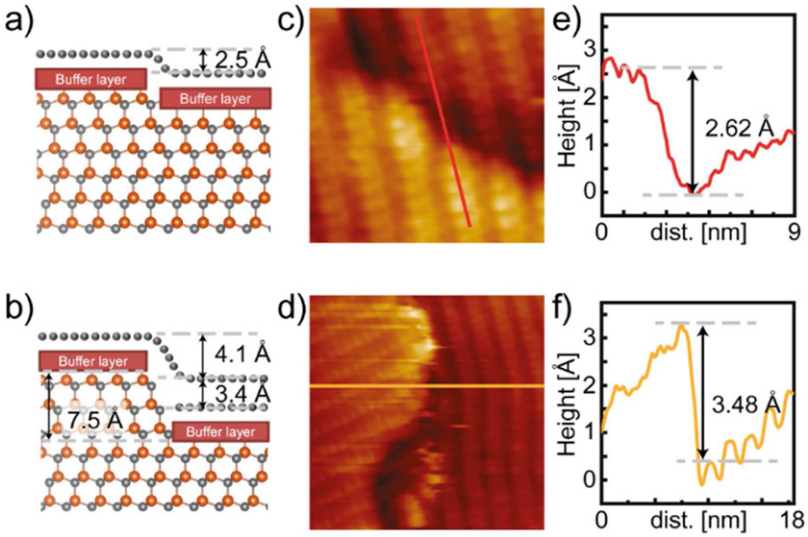


**Figure 4.** Line profiles across the step edges. (a), (b) Atomic structure models of the step edges between (a) single-layer graphene domains and (b) single-layer and bilayer graphene domains, with the orange and gray spheres representing the Si and C atoms. (c), (d) STM images of the flat-lying structures on the step edges between (c) single-layer graphene domains and (d) single-layer and bilayer graphene domains. (e), (f) Height profiles measured along the lines in (c) and (d), respectively.

single-layer graphene, as reported previously [31]. The results suggest that the interactions of pentacene molecules with graphene become weaker when the number of graphene layers increases. Some carbon atoms of zero-layer graphene have localized unsaturated dangling bonds, which induces strong interactions with the pentacene molecules [31]. The single-layer graphene is affected by the underlying zero-layer graphene with localized unsaturated dangling bonds, where the effects are reduced when the number of graphene layers increase. Therefore, the localized unsaturated dangling bonds of the zero-layer graphene may be a major contribution to the strength of the interactions of pentacene molecules with graphene.

The main differences between the single-layer and bilayer step edges are their heights and chemical configurations. Hence, there are two possible origins for the limited step-crossing arrangement at the bilayer step edges. First, the steepness of the step edge could be a limiting factor for the step-crossing arrangement. The curved geometry at both the end and beginning of the step structure could disturb the interactions between the graphene and pentacene molecules when the pentacene molecules are in the flat-lying arrangement. Second, the underlying chemical configuration of the single-layer step edge is uniform. In contrast to this, in the bilayer step edge, the electron-doped, semiconducting, bilayer graphene is connected to the electron-doped, metallic, single-layer graphene. Furthermore, the first layer of the bilayer graphene is terminated at the step edge, which can leave an unsaturated dangling bond. These chemical changes at the step edge could alter the interactions between the graphene and pentacene molecules [50, 51].

## 4. Conclusion

The effects of various imperfections on the structure of self-assembled pentacene molecules grown on epitaxial graphene was studied with STM, with the pentacene molecules forming a flat-lying structure when they are one layer thick and a herringbone structure when they are multiple layers thick. The typical defects found in epitaxial graphene grown on SiC(0001), subsurface CNT defects and step edges, were considered in the study. The subsurface CNT defects disturbed the flat-lying structure locally, but the overall arrangement was maintained. The effects of the subsurface CNT defects were weakened with the multilayer-thick pentacene, and therefore, the herringbone structure was not influenced by the subsurface CNT defects. The most important effects were found at the step edges. When a step edge was formed between single-layer graphene domains, the pentacene molecules were unaffected and grew continuously across the step edge. In contrast to the single-layer step edge, the bilayer step edge limited the continuous growth and degraded the quality of the pentacene film significantly. This study suggests that the uniformity of the graphene layer is the most important factor in the growth of high-quality pentacene films on epitaxial graphene, while the other imperfections have negligible effects.

## Acknowledgments

This study was supported by a grant from the National Research Foundation of Korea (NRF-2015R1A2A2A01004853)

## References

[1] Geim A K and Novoselov K S 2007 The rise of graphene *Nat. Mater.* **6** 183–91
[2] Jeon C *et al* 2013 Opening and reversible control of a wide energy gap in uniform monolayer graphene *Sci. Rep.* **3** 2725
[3] Park J-H, Cho D-H, Moon Y, Shin H-C, Ahn S-J, Kwak S K, Shin H-J, Lee C and Ahn J R 2014 Designed 3D freestanding single-crystal carbon architectures *ACS Nano* **8** 11657

[4] Shin H-C *et al* 2015 Epitaxial growth of a single-crystal hybridized boron nitride and graphene layer on a wide-band gap semiconductor *J. Am. Chem. Soc.* **137** 6897

[5] Bonaccorso F, Sun Z, Hasan T and Ferrari A C 2010 Graphene photonics and optoelectronics *Nat. Photonics* **4** 611–22

[6] Wu J, Agrawal M, Becerril A, Bao Z, Liu Z, Chen Ḱ Y and Peumans P 2010 Organic light-emitting diodes on solution-processed graphene transparent electrodes *ACS Nano* **4** 43–8

[7] Han T-H, Lee Y, Choi M-R, Woo S-H, Bae S-H, Hong B H, Ahn J-H and Lee T-W 2012 Extremely efficient flexible organic light-emitting diodes with modified graphene anode *Nat. Photon.* **6** 105–10

[8] Kang S J, Kim B, Kim K S, Zhao Y, Chen Z, Lee G H, Hone J, Kim P and Nuckolls C 2011 Inking elastomeric stamps with micro-patterned, single layer graphene to create high-performance OFETs *Adv. Mater.* **23** 3531–5

[9] Di C A, Wei D, Yu G, Liu Y, Guo Y and Zhu D 2008 Patterned graphene as source/drain electrodes for bottom-contact organic field-effect transistors *Adv. Mater.* **20** 3289–93

[10] Lee S, Jo G, Kang S J, Wang G, Choe M, Park W, Kim D Y, Kahng Y H and Lee T 2011 Enhanced charge injection in pentacene field-effect transistors with graphene electrodes *Adv. Mater.* **23** 100–5

[11] Lee W H, Park J, Sim S H, Jo S B, Kim K S, Hong B H and Cho K 2011 Transparent flexible organic transistors based on monolayer graphene electrodes on plastic *Adv. Mater.* **23** 1752–6

[12] Lee W H, Park J, Sim S H, Lim S, Kim K S, Hong B H and Cho K 2011 Surface-directed molecular assembly of pentacene on monolayer graphene for high-performance organic transistors *J. Am. Chem. Soc.* **133** 4447–54

[13] Berke K, Tongay S, McCarthy M A, Rinzler A G, Appleton B R and Hebard A F 2012 Current transport across the pentacene/CVD-grown graphene interface for diode applications *J. Phys.: Condens. Matter* **24** 255802

[14] Gomez De Arco L, Zhang Y, Schlenker C W, Ryu K, Thompson M E and Zhou C 2010 Continuous, highly flexible, and transparent graphene films by chemical vapor deposition for organic photovoltaics *ACS Nano* **4** 2865–73

[15] Park H, Rowehl J A, Kim K K, Bulovic V and Kong J 2010 Doped graphene electrodes for organic solar cells *Nanotechnology* **21** 505204

[16] Jurchescu O D, Baas J and Palstra T T M 2004 Effect of impurities on the mobility of single crystal pentacene *Appl. Phys. Lett.* **84** 3061–3

[17] Minari T, Nemoto T and Isoda S 2004 Fabrication and characterization of single-grain organic field-effect transistor of pentacene *J. Appl. Phys.* **96** 769–72

[18] Coropceanu V, Cornil J, da Silva Filho D A, Olivier Y, Silbey R and Brèdas J L 2007 Charge transport in organic semiconductors *Chem. Rev.* **107** 926–52

[19] Brédas J L, Calbert J P, da Silva Filho D A and Cornil J 2002 Organic semiconductors: a theoretical characterization of the basic parameters governing charge transport *Proc. Natl Acad. Sci. USA* **99** 5804–9

[20] Stadler C, Hansen S, Kröger I, Kumpf C and Umbach E 2009 Tuning intermolecular interaction in long-range-ordered submonolayer organic films *Nat. Phys.* **5** 153–8

[21] Kronik L and Morikawa Y 2013 *The Molecule-Metal Interface* ed N Kock *et al* (New York: Wiley) pp 51–89

[22] Lauffer P, Emtsev K V, Graupner R, Seyller T and Ley L 2008 Molecular and electronic structure of PTCDA on bilayer graphene on SiC(0 0 0 1) studied with scanning tunneling microscopy *Phys. Status Solidi* **245** 2064–7

[23] Wang Q H and Hersam M C 2009 Room-temperature molecular-resolution characterization of self-assembled organic monolayers on epitaxial graphene *Nat. Chem.* **1** 206–11

[24] Huang H, Chen S, Gao X, Chen W and Wee A T S 2009 Structural and electronic properties of PTCDA thin films on epitaxial graphene *ACS Nano* **3** 3431–6

[25] Pollard A J *et al* 2010 Supramolecular assemblies formed on an epitaxial graphene superstructure *Angew. Chem. Int. Ed. Engl.* **49** 1794–9

[26] Yang H, Mayne A J, Comtet G, Dujardin G, Kuk Y, Sonnet P, Stauffer L, Nagarajan S and Gourdon A 2013 STM imaging, spectroscopy and manipulation of a self-assembled PTCDI monolayer on epitaxial graphene *Phys. Chem. Chem. Phys.* **15** 4939–46

[27] Barja S, Garnica M, Hinarejos J J, Vázquez de Parga A L, Martín N and Miranda R 2010 Self-organization of electron acceptor molecules on graphene *Chem. Commun. (Camb.)* **46** 8198–200

[28] Garnica M, Stradi D, Barja S, Calleja F, Diaz C, Alcami M, Martin N, Parga A L V, Martin F and Miranda R 2013 Long-range magnetic order in a purely organic 2D layer adsorbed on epitaxial graphene *Nat. Phys.* **9** 368–74

[29] Yang K, Xiao W D, Jiang Y H, Zhang H G, Liu L W, Mao J H, Zhou H T, Du S X and Gao H J 2012 Molecule–substrate coupling between metal phthalocyanines and epitaxial graphene grown on Ru(0 0 0 1) and Pt(1 1 1) *J. Phys. Chem.* C **116** 14052–6

[30] Wang Y-L *et al* 2010 Selective adsorption and electronic interaction of $F_{16}$CuPc on epitaxial graphene *Phys. Rev.* B **82** 245420

[31] Jung W, Oh D-H, Song I, Shin H-C, Ahn S J, Moon Y, Park C-Y and Ahn J R 2014 Influence of graphene-substrate interactions on configurations of organic molecules on graphene: pentacene/epitaxial graphene/SiC *Appl. Phys. Lett.* **105** 071606

[32] Jee H G, Han J H, Hwang H N, Kim B, Kim H S, Kim Y D and Hwang C C 2009 Pentacene as protection layers of graphene on SiC surfaces *Appl. Phys. Lett.* **95** 093107

[33] Zhang H G *et al* 2011 Assembly of iron phthalocyanine and pentacene molecules on a graphene monolayer grown on Ru(0 0 0 1) *Phys. Rev.* B **84** 245436

[34] Shi C, Wei C, Han H, Xingyu G, Dongchen Q, Yuzhan W and Wee A T S 2010 Template-directed molecular assembly comparison between CuPc and pentacene *ACS Nano* **4** 849–54

[35] Zhou H T, Mao J H, Li G, Wang Y L, Feng X L, Du S X, Müllen K and Gao H J 2011 Direct imaging of intrinsic molecular orbitals using 2D, epitaxially-grown, nanostructured graphene for study of single molecule and interactions *Appl. Phys. Lett.* **99** 153101

[36] Huang H, Chen W, Chen S and Wee A T S 2008 Bottom-up growth of epitaxial graphene on 6H-SiC(0 0 0 1) *ACS Nano* **2** 2513–8

[37] Choi J, Lee H and Kim S 2010 Atomic-scale investigation of epitaxial graphene grown on 6H-SiC (0 0 0 1) using scanning tunneling microscopy and spectroscopy *J. Phys. Chem.* C **114** 13344–8

[38] Hibino H, Tanabe S, Mizuno S and Kageshima H 2012 Growth and electronic transport properties of epitaxial graphene on SiC *J. Phys. D: Appl. Phys.* **45** 154008

[39] Cockayne E, Rutter G M, Guisinger N P, Crain J N, First P N and Stroscio J A 2011 Grain boundary loops in graphene *Phys. Rev.* B **83** 195425

[40] Derycke V, Martel R, Radosavljević M, Ross F M and Avouris Ph 2002 Catalyst-free growth of ordered single-walled carbon nanotube networks *Nano Lett.* **2** 1043–6

[41] Mattheus C C, de Wijs G A, de Groot R A and Palstra T T M 2003 Modeling the polymorphism of pentacene *J. Am. Chem. Soc.* **125** 6323–30

[42] Chen W, Huang H, Thye A and Wee S 2008 Molecular orientation transition of organic thin films on graphite:

the effect of intermolecular electrostatic and interfacial dispersion forces *Chem. Commun. (Camb.)* **2008** 4276–8
[43] Emery J D, Wang Q H, Zarrouati M, Fenter P, Hersam M C and Bedzyk M J 2011 Structural analysis of PTCDA monolayers on epitaxial graphene with ultra-high vacuum scanning tunneling microscopy and high-resolution x-ray reflectivity *Surf. Sci.* **605** 1685–93
[44] Gavioli L, Fanetti M, Sancrotti M and Betti M G 2005 Long-range-ordered pentacene chains assembled on the Cu(1 1 9) vicinal surface *Phys. Rev.* B **72** 035458
[45] Gavioli L, Fanetti M, Pasca D, Padovani M, Sancrotti M and Betti M G 2004 Quasi-1D pentacene structures assembled on the vicinal Cu(1 1 9) surface *Surf. Sci.* **566–568** 624–7
[46] Götzen J, Käfer D, Wöll C and Witte G 2010 Growth and structure of pentacene films on graphite: weak adhesion as a key for epitaxial film growth *Phys. Rev.* B **81** 085440
[47] Hupalo M, Conrad E H and Tringides M C 2009 Growth mechanism for epitaxial graphene on vicinal 6H-SiC (0 0 0 1) surfaces: a scanning tunneling microscopy study *Phys. Rev.* B **80** 041401(R)
[48] Ye M, Cui Y T, Nishimura Y, Yamada Y, Qiao S, Kimura A, Nakatake M, Namatame H and Taniguchi M 2010 Edge states of epitaxially grown graphene on 4H-SiC(0 0 0 1) studied by scanning tunneling microscopy *Eur. Phys. J.* B **75** 31–5
[49] Ohta T, Bartelt N C, Nie S, Thürmer K and Kellogg G L 2010 Role of carbon surface diffusion on the growth of epitaxial graphene on SiC *Phys. Rev.* B **81** 121411(R)
[50] Wang X, Tabakman S and Dai H 2008 Atomic layer deposition of metal oxides on pristine and functionalized graphene *J. Am. Chem. Soc.* **130** 8152–3
[51] Acik M and Chabal Y J 2011 Nature of graphene edges: a review *Japan. J. Appl. Phys.* **50** 070101